Available online at www.sciencedirect.com
ScienceDirect
Journal of Power Sources 177 (2008) 631–636
JOURNAL OF POWER SOURCES
www.elsevier.com/locate/jpowsour

Short communication

Low-Pt-loading acetylene-black cathode for high-efficient dye-sensitized solar cells

Fengshi Cai [a,c], Jing Liang [a], Zhanliang Tao [a], Jun Chen [a,*], Ruisong Xu [b]

[a] *Institute of New Energy Material Chemistry, Nankai University, Tianjin 300071, PR China*
[b] *Guangzhou Institute of Geochemistry, Chinese Academy of Science, Guangzhou 510640, PR China*
[c] *College of Materials Science and Engineering, Tianjin University of Technology, Tianjin 300191, PR China*

Received 22 April 2007; received in revised form 4 September 2007; accepted 28 October 2007
Available online 28 November 2007

Abstract

We reported on the synthesis, characterization, and photovoltaic/electrochemical properties of Pt/acetylene-black (AB) cathode as well as their application in dye-sensitized solar cells (DSCs). The Pt/AB electrode was prepared through a thermal decomposition of H_2PtCl_6 on the AB substrate. SEM and TEM observations showed that the Pt nanoparticles were homogeneously dispersed on the AB surface. The Pt-loading content in the Pt/AB electrode was only about 2.0 $\mu g\,cm^{-2}$, which was much lower than 5–10 $\mu g\,cm^{-2}$ generally used for the Pt electrode in DSCs. Electrochemical measurements displayed a low charge-transfer resistance of 1.48 $\Omega\,cm^2$ for the Pt/AB electrode. Furthermore, when this low-Pt-loading electrode was used as the cathode of DSCs, an overall light-to-electricity energy conversion efficiency of 8.6% was achieved, showing commercially realistic energy conversion efficiency in the application of DSCs.

Keywords: Dye-sensitized solar cells; Acetylene-black; Pt; Light-to-electricity conversion efficiency

1. Introduction

The dye-sensitized solar cells (DSCs) have attracted much attention in transferring clean solar energy to electricity because of their low cost, easy production and relatively high efficiency (8–11%) [1]. In general, DSCs are composed of a dye-sensitized TiO_2 photoanode, a Pt cathode (counter electrode, CE), and an electrolyte containing a redox couple (I^-/I_3^-). One of the critical components of DSCs is the cathode that plays an important role for the catalytic I_3^- reduction and electron transfer [2]. To obtain the desired catalytic effect, noble-metal Pt is usually employed as the CE of DSCs, in which the amount of Pt is about 5–10 $\mu g\,cm^{-2}$ [3].

As an alternative to the Pt in DSCs, carbon-based materials including carbon film [4], carbon nanotubes [5], carbon black [6], activated carbon [7] and C_{60} thin films [8] were used as the CE of DSCs. However, these Pt-free CEs usually require a thick porous film to obtain an acceptable catalytic effect, and the conversion efficiency is relatively low compared to that of Pt. Recently, new CEs such as Pt–NiO, Pt–SnO_2–Sb were reported, which can increase the active surface area of Pt and also reduce the manufacturing cost [9,10], revealing that highly distributed Pt nanoparticles with small size on the substrate are ideal for high electrocatalytic activity.

Acetylene-black (AB), which has been intensively studied in battery systems [11,12], has excellent electric conductivity, large specific surface area and strong adsorptive ability. In our previous study, it was found that pure AB was suitable as the CE of DSCs [13]. Here, we report on the preparation of Pt/AB with low Pt loading of 2.0 $\mu g\,cm^{-2}$ and their high electrocatalytic activity in DSCs. In particular, an overall light-to-electricity energy conversion efficiency of 8.6% was obtained for the DSCs with Pt/AB, indicating the potential application in DSCs.

2. Experimental

2.1. Preparation of TiO_2 photoanode

Nanocrystalline TiO_2 film was prepared according to the reported method [14]. The fluorine-doped SnO_2 conducting glass (FTO) (10 $\Omega\,\square^{-1}$, Nippon Sheet Glass) was first treated

* Corresponding author. Tel.: +86 22 23506808; fax: +86 22 23509118.
E-mail address: chenabc@nankai.edu.cn (J. Chen).

0378-7753/$ – see front matter © 2007 Elsevier B.V. All rights reserved.
doi:10.1016/j.jpowsour.2007.10.096

with 50 mM $TiCl_4$ aqueous solution at 70 °C for 30 min. The paste consisting of 16.2% TiO_2 (P25 Degussa) and 4.5% ethyl cellulose in terpineol was deposited onto the $TiCl_4$-pretreated conducting glass using a screen printing technique. The resulting layer was sintered in the air at 450 °C for 30 min before cooling to room temperature. The heated electrodes were impregnated with 50 mM $TiCl_4$ aqueous solution in a water-saturated desiccator at 70 °C for 30 min and then washed with distilled water for several times. Immediately, before being dipped into the dye solution, it was fired again at 450 °C for 30 min in the air and then cooled to 80 °C. Finally, the TiO_2 electrode was immersed into 3×10^{-4} M ruthenium polypyridyl complex N3 dye ethanol solution at room temperature for overnight to afford sensitization. The resulting film thickness was about 12 μm.

2.2. Preparation of AB, Pt, Pt/AB, Pt/TiO_2 counter electrode

The AB, Pt/AB or Pt/TiO_2 counter electrode was prepared by a doctor blade technique. The preparation of AB powder was described in Ref. [13]. The conductivity of the acetylene film is 0.6 S cm^{-1}. To obtain the AB paste, 130 mg of AB powder was mixed with 4.5% ethyl cellulose in 2.5 mL terpineol. Then the paste was coated on FTO-glass by doctor-blading. The Pt nanoparticles were produced by thermal decomposition of H_2PtCl_6 (2 mM in water) on AB or TiO_2 film at 385 °C for 30 min. The thickness of the films was controlled by the height of two adhesive tape strips, which were attached on two parallel ends of the FTO surface. After dried in the air, the films were calcined in the air at 450 °C for 30 min to remove the organic content and form a three-dimensional network. The thickness of the as-prepared films was about 5 μm. As a comparison, the Pt/FTO electrode was prepared by thermal decomposition of H_2PtCl_6 (30 mM in isopropanol) on FTO-glass at 385 °C for 30 min. The amount of Pt with 2.0 μg cm^{-2} in Pt/AB electrode gives 2.0 μg Pt for 5 μm (thickness) × 1 cm^2 volume in the AB layer. The as-synthesized thickness of this film was about 5 μm with an electrode area of 0.25 cm^2.

2.3. Assembly of the DSC

DSCs were fabricated by using the dye-sensitized nanoporous TiO_2 photoanode and the AB, Pt, Pt/AB or Pt/TiO_2 counter electrode, as shown in Fig. 1. The liquid electrolyte, which is a solution of 0.6 M of 1,2-dimethyl-3-propylimidazolium iodide (DMPImI), 0.1 M of LiI, 0.05 M of I_2 and 0.5 M of *t*-butylpyridine (tBP) in a mixture of acetonitrile/methoxypropionitrile (volume ratio = 1:1), was firstly dropped on the dye-sensitized nanoporous TiO_2 films and then the photoanode was clipped firmly with counter electrode. The area of the TiO_2 photoelectrode was 0.16 cm^2.

2.4. Characterization and measurements

The Pt loading in the as-prepared specimens was determined by an inductively coupled plasma (ICP) atomic emission spectroscopy (model P-5200 from Hitachi). For the ICP analysis,

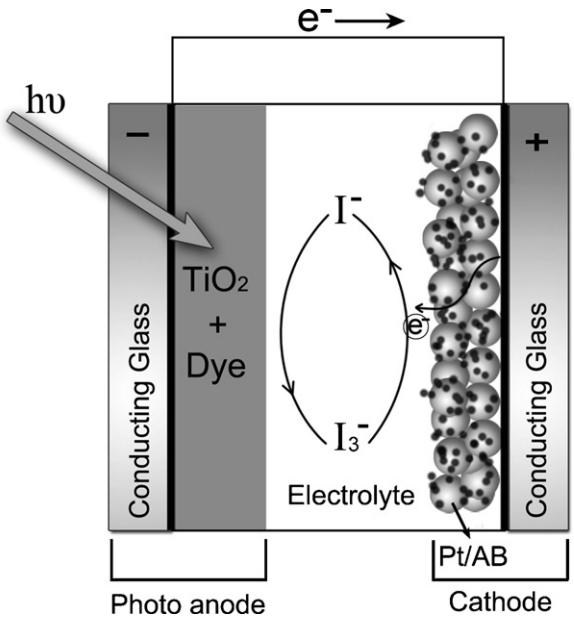

Fig. 1. Scheme of the cross-sectional view for the dye-sensitized solar cells with the TiO_2 photoanode and the Pt/AB counter electrode.

the as-prepared Pt loading electrode was placed in aqua regia with vigorous agitation for 48 h to completely dissolve the Pt. The morphologies and microstructures of the Pt/AB films were characterized by scanning electron microscope (SEM, Philips XL-30), transmission electron microscope (TEM), and high-resolution TEM (HRTEM) (Philips Tecnai 20, 200 kV). The specific surface areas of the AB-based films were measured by nitrogen gas adsorption/desorption methods with Shimadzu-Micromeritics ASAP 2010 Instrument.

Photoelectrochemical data were carried out using a 500-W xenon light source that was focused to give 100 mW cm^{-2} the equivalent of one sun at AM 1.5. The spectral output of the lamp was matched in the region of 400–800 nm with the aid of a sunlight filter. The applied potential and cell currents were measured using a Keithley model 2400 digital source meter (Keithley, USA) at room temperature. The conversion efficiency (η) of the DSCs is calculated from the short current density (J_{sc}), the open voltage (V_{oc}), the fill factor of the cell (ff), and the intensity of the incident light (I_s) by Ref. [15]:

$$\eta = \frac{J_{sc} V_{oc} \mathrm{ff}}{I_s} \quad (1)$$

The electrochemical impedance was investigated by means of a PARSTAT 2273 instrument at 25 °C in the frequency range of 10^{-2} to 10^5 Hz. The electrical impedance spectra were characterized by using Zsimpwin software in terms of the proposed equivalent circuit. The distance between the two electrodes was about 45 μm.

3. Results and discussion

Fig. 2a shows the typical SEM image of the as-prepared Pt/AB, displaying a porous-structure character with the AB diameter of approximately 50–100 nm. The detailed morphol-

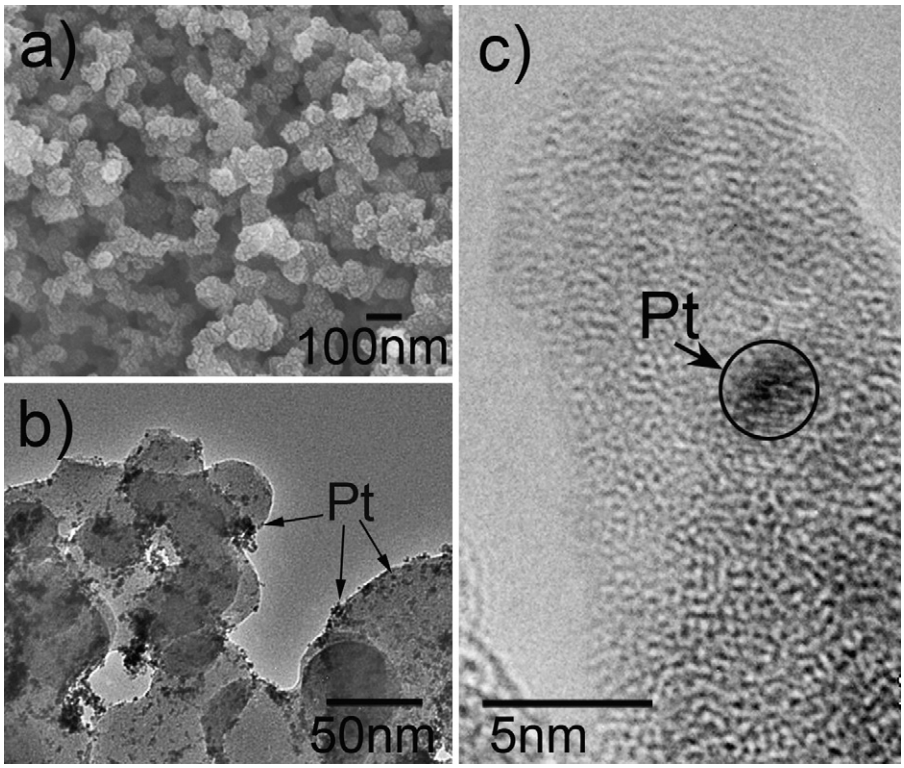

Fig. 2. (a) SEM, (b) TEM, and (c) HRTEM images of the as-synthesized Pt/AB.

ogy and microstructure of the Pt-deposited AB is further characterized by TEM (b) and HRTEM (c). It is observed that the Pt nanoparticles with the diameter of 2–4 nm were distributed over the AB substrate. The specific surface areas of the porous AB and Pt/AB were 280 and 316 $m^2\,g^{-1}$, respectively. The Pt/AB composite structure is considered to be more efficient for Pt usage than that of the pure Pt electrode due to the depression of the particle aggregations and the formation of more Pt/AB/electrolyte surface/interface boundaries [16].

In order to examine the catalytic activity of the Pt/AB electrode, electrochemical impedance spectroscopy (EIS) was investigated. The total reaction at the Pt/AB/electrolyte interface is: $I_3^- + 2e^- = 3I^-$. The charge-transfer resistance (R_{ct}) of the Pt/AB is a value of its catalytic activity for reducing the triiodide ion. In this case, the reaction species, I_3^- ions, must enter into pores of the AB films, and further have to be reduced to the I^- in the pores by capturing the electrons that migrate from the external circuit. The I^- regenerated in the cathode must diffuse through the liquid contained in the pores of the porous layers to the photoelectrode [17].

Fig. 3 shows the impedance spectra of the sandwich type cells with a Pt/AB and Pt/FTO-glass electrodes. Three semicircles were observed in the measured frequency range of 0.01 to 10^5 Hz (Fig. 3a). The first high frequency semicircle (in the region of 10^3 to 10^5 Hz) and the second semicircle (in the frequency region of 10 to 10^3 Hz) can be interpreted as the charge-transfer process at the Pt electrode/electrolyte interface and the Pt/AB electrode/electrolyte interface, respectively. While the third semicircle around 1 Hz represents the Warburg impedance for triiodide diffusion in the electrolyte. Fig. 3c shows the Nyquist plot of Pt/FTO electrodes with various Pt loading. From Fig. 3c, R_{ct} of 0.92, 1.03, 1.37and 1.75 $\Omega\,cm^2$ can be deduced for a Pt content of 6.5, 5.0, 3.7 and 2.2 $\mu g\,cm^{-2}$, respectively, being an index of the catalytic performance of the Pt electrode. This result reveals that porous Pt/AB films provide more interface between the Pt/AB and the electrolyte.

Fig. 4 shows the variation of electrocatalytic activity with Pt loading for Pt/AB electrode. It can be seen that the R_{ct} decreases with the increase of Pt loading. However, the charge-transfer resistance keeps nearly constant when the Pt loading exceeds 2.0 $\mu g\,cm^{-2}$. The SEM investigation shows that Pt nanoparticles in the AB film are located compactly to each other and tend to form bigger particles with the increase of Pt loading (higher than 2.0 $\mu g\,cm^{-2}$). Taking into account the high electrocatalytic activity and the low cost of the counter electrode for DSCs applications, Pt loading of 2.0 $\mu g\,cm^{-2}$ was adopted in the preparation of the Pt/AB electrode.

Fig. 5 shows the *I–V* curves of the DSCs based on various counter electrodes of Pt/TiO_2, AB, Pt/AB and Pt. Table 1 summarizes the properties (J_{sc}, V_{oc}, ff, η) of the DSCs. It can be seen that the DSCs with Pt/AB (with 2.0 and 3.8 $\mu g\,cm^{-2}$ Pt, respectively) and Pt electrodes exhibit a relatively higher conversion efficiency of 8.6%, 9.0% and 8.3%, respectively. On the other hand, the DSCs based on AB and Pt/TiO_2 electrodes show the conversion efficiency of 4.3% and 1.3%, respectively. This result indicates that Pt/AB is feasible in DSCs with high conversion efficiency. Compared to the properties of the DSCs with Pt/TiO_2, the most pronounced change for the use of Pt/AB is the short circuit current densities (J_{sc}) and fill factor (ff). The J_{sc} increases from 11.8 to 20.7 mA cm^{-2} and the ff enhances from

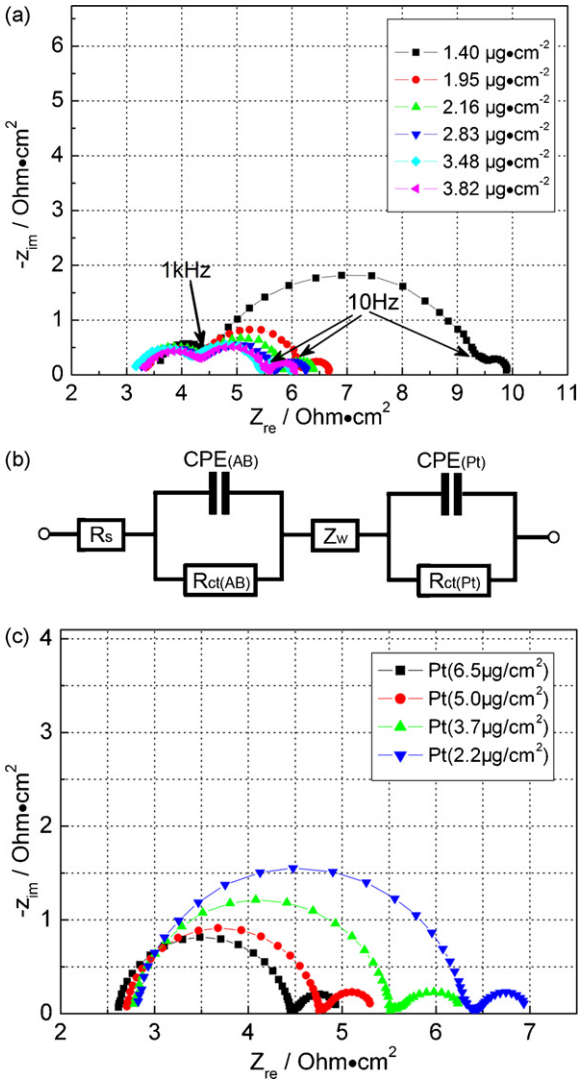

Fig. 3. (a) Nyquist plots for the electrochemical cells consisting of a Pt/AB electrode with different Pt loading. (b) Equivalent circuit for the impedance spectrum. R_{ct} (Pt) or R_{ct} (AB): charge-transfer resistance; R_s: serial resistance; CPE(Pt) or CPE(AB): constant phase element; Z_W: Warburg impedance (diffusion impedance). (c) Nyquist plot of Pt/FTO electrodes with various Pt loading.

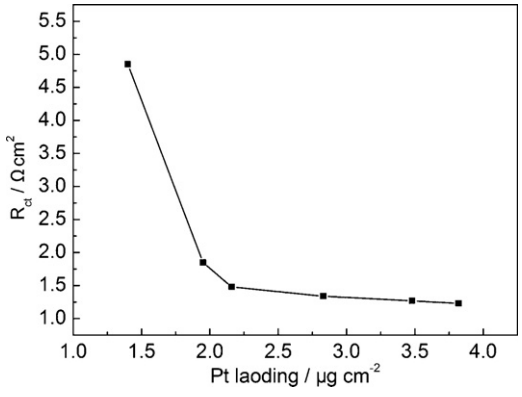

Fig. 4. The charge-transfer resistance R_{ct} of Pt/AB electrodes with different Pt loading.

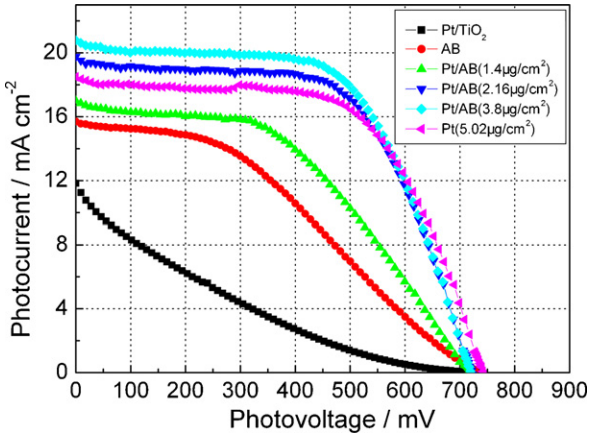

Fig. 5. Photocurrent (I)–voltage (V) curves of DSCs with Pt/TiO_2, AB, Pt/AB and Pt electrodes under AM 1.5–100 mW cm^{-2} light irradiation.

Table 1
Photoelectric performances of the cells in Fig. 5

Counter electrodes	Pt-loading (μg cm^{-2})	J_{sc} (mA cm^{-2})	V_{oc} (mV)	ff (%)	η (%)
Pt/TiO_2	1.85[a]	11.8	729	15.6	1.3
AB	0	15.7	728	37.5	4.3
Pt/AB	1.4[a]	16.9	721	45.8	5.5
Pt/AB	2.16[a]	19.8	723	60.1	8.6
Pt/AB	3.8[a]	20.7	721	60.4	9.0
Pt	5.02	18.5	742	60.5	8.3

[a] Value calculated based on film thickness of 5 μm.

15.6% to 60.4%, which can be attributed to an addition of AB in the electrode, owing to a decrease of the internal resistance (in Table 2) and an increase of the active surface area by depositing Pt nanoparticles in the AB support. For the Pt/AB electrode, it was observed that the short circuit current (I_{sc}), fill factor (ff) and conversion efficiency (η) increases with an increase of Pt loading. However, the cell performance keeps nearly constant when the Pt loading exceeds 2.0 μg cm^{-2}. This fact agrees with our previous discussion that the Pt loading affects the R_{ct} greatly. Moreover, the amount of Pt with 2.0 μg cm^{-2} in Pt/AB electrode is considerably lower than that of 5–10 μg cm^{-2} commonly used for DSCs. Obviously, the highly dispersed Pt/AB with a low Pt loading provides the possibility of cost reduction in DSCs manufacturing process.

Fig. 6 shows the Nyquist plots for the electrochemical cells fitted to the simulated equivalent circuit shown in Fig. 3b. For the Pt/TiO_2 and AB counter electrodes, a large arch is visible in the low frequency region of the Nyquist diagram (Figs. 6a and b), which is due to the impaired electron transfer at the counter electrode. While the arch for the electrolyte diffusion is hidden by the large charge-transfer resistance on the Pt/TiO_2 and AB. However, the charge-transfer resistance for the Pt/AB (with 2.0 μg cm^{-2} Pt) becomes so small that a third semicircle representing the Warburg impedance for triiodide diffusion emerges (Fig. 6c). The fitting results are summarized in Table 2. The Pt/TiO_2 electrode shows an extremely high R_{ct} of above 1000 Ω cm^2, while the electrode of AB shows a R_{ct} of 75 Ω cm^2. This leads to the lower ff and reduces the cell efficiency due to the

Table 2
Impedance parameters of the various counter electrodes estimated from the impedance spectra in Fig. 6 and equivalent circuit in Fig. 3b

CE type	Pt-loading ($\mu g\,cm^{-2}$)	R_{ct} ($\Omega\,cm^2$)	CPE(CE):B($S\,s^{\beta}$)	CPE(CE):β	R_s ($\Omega\,cm^2$)
Pt	5.02	1.03	4.34×10^{-6}	0.93	2.57
Pt/AB	2.16	1.48	2.15×10^{-4}	0.85	3.27
AB	0	75	2.99×10^{-4}	0.92	3.55
Pt/TiO_2	1.85	1150	9.12×10^{-4}	0.93	3.98

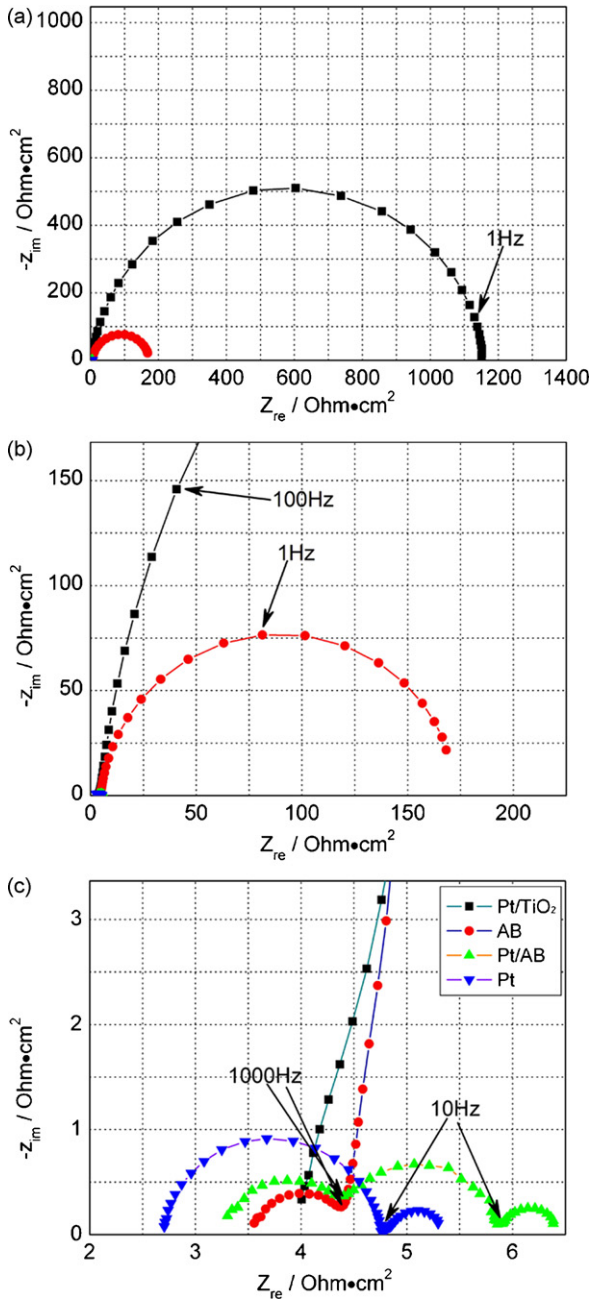

Fig. 6. (a) Nyquist plots of the electrochemical cells consisting of a Pt/FTO-glass and various catalytic layer-coated FTO-glasses as working electrodes; (b) and (c) are the expanded ranges of 0–200 $\Omega\,cm^2$ and 2–7 $\Omega\,cm^2$, respectively.

high R_{ct}. For the CE of AB, the conversion efficiency of the cells is still insufficient (4.3%) and should be increased to more than 8% for practical usage [6]. Thus, small amount Pt nanoparticles are deposited on AB in order to improve its catalytic ability. The results show that the R_{ct} of the AB electrode with the loading of Pt nanoparticles decreases sharply from 75 to 1.48 $\Omega\,cm^2$ and approaches the R_{ct} value of 1.03 $\Omega\,cm^2$, which is promising for application.

In the Nyquist plots, the impedance spectrum of Pt appears generally in the region of 1–100 kHz, while the use of porous Pt/AB-based film lowers the frequency range of the response to 0.01–1 kHz. The depression of the semicircle to an ellipse is caused owing to the porous structure of the electrodes. This effect can be described by a constant phase element (CPE) [6,17]. The impedance Z_{CPE} of a CPE is

$$Z_{CPE} = B(j\omega)^{-\beta} \quad (0 \le \beta \le 1) \tag{2}$$

where ω is the angular frequency, B is the CPE parameter and β is the CPE exponent. B indicates the capacitance of CPE and the deviation from the semicircle probably due to the porosity of electrode surface, respectively. In the case of $\beta = 1$ in Eq. (2), the CPE shows a perfect capacitor, exhibiting an exact semicircle in the Nyquist plots. While the semicircle is depressed in the case of $\beta < 1$ due to the porosity of electrode surface. Compared with that of Pt, the CPE exponent (β) of the Pt/AB is smaller. Therefore, the Pt/AB electrodes with 2.0 $\mu g\,cm^{-2}$ Pt-loading appears the same low charge-transfer resistance as that of Pt electrode with 5.02 $\mu g\,cm^{-2}$ Pt-loading. Meanwhile, the high active surface in the Pt/AB decreases the R_{ct} of the CE and improves the cell performance.

4. Conclusions

The Pt/AB electrode with low Pt loading of 2.0 $\mu g\,cm^{-2}$ can reach the promising photovoltaic performances, which were almost comparable to that of pure Pt/FTO glass with Pt loading of 5.02 $\mu g\,cm^{-2}$. A light-to-electricity energy conversion efficiency of 8.6% was achieved for the DSCs with the Pt/AB electrode. Electrochemical measurements showed that the Pt/AB composite had lower charge-transfer resistance and higher catalytic activity than that of pure Pt. This work should be useful for reducing the manufacturing costs of DSCs.

Acknowledgements

This work was supported by the National MOST Program (2005CB623607 and 2007AA05Z124) and TJKJ 07ZCGHHZ00700.

References

[1] M. Grätzel, Nature 414 (2001) 338–344.
[2] N. Papageorgiou, Coord. Chem. Rev. 248 (2004) 1421–1446.
[3] N. Papageorgiou, W.F. Maier, M. Grätzel, J. Electrochem. Soc. 144 (1997) 876–884.
[4] A. Kay, M. Grätzel, Sol. Energy Mater. Sol. Cells 44 (1996) 99–117.
[5] K. Suzuki, M. Yamaguchi, M. Kumagai, S. Yanagida, Chem. Lett. 32 (2003) 28–29.
[6] T.N. Murakami, S. Ito, Q. Wang, M.K. Nazeeruddin, T. Bessho, I. Cesar, P. Liska, R. Humphry-Baker, P. Comte, P. Péchy, M. Grätzel, J. Electrochem. Soc. 153 (2006) A2255–A2261.
[7] K. Imoto, K. Takatashi, T. Yamaguchi, T. Komura, J. Nakamura, K. Murata, Sol. Energy Mater. Sol. Cells 79 (2003) 459–469.
[8] T. Hino, Y. Ogawa, N. Kuramoto, Carbon 44 (2006) 880–887.
[9] S.S. Kim, K.W. Park, J.H. Yum, Y.E. Sung, Sol. Energy Mater. Sol. Cells 90 (2006) 283–290.
[10] G. Khelashvili, S. Behrens, C. Weidenthaler, C. Vetter, A. Hinsch, R. Kern, K. Skupien, E. Dinjus, H. Bönnemann, Thin Solid Films 511/512 (2006) 342–348.
[11] M. Wissler, J. Power Sources 156 (2006) 142–150.
[12] W.Y. Li, C.S. Li, C.Y. Zhou, H. Ma, J. Chen, Angew. Chem. Int. Ed. 45 (2006) 6009–6012.
[13] F.S. Cai, J. Chen, R.S. Xu, Chem. Lett. 35 (2006) 1266–1267.
[14] P. Wang, S.M. Zakeeruddin, P. Comte, R. Charvet, R.H. Baker, M. Grätzel, J. Phys. Chem. B 107 (2003) 14336–14341.
[15] A. Hagfeldt, M. Gratzel, Acc. Chem. Res. 33 (2000) 269–277.
[16] M. Kim, J.N. Park, H. Kim, S. Song, W.H. Lee, J. Power Sources 163 (2006) 93–97.
[17] A. Hauch, A. Georg, Electrochim. Acta 46 (2001) 3457–3466.